

Unilateral Fixtures for Sheet-Metal Parts With Holes

Kanakasabapathi Gopalakrishnan, Ken Goldberg, *Senior Member, IEEE*, Gary M. Bone, Matthew J. Zaluzec, Rama Koganti, Rich Pearson, and Patricia A. Deneszcuk

Abstract—In this paper, we introduce *unilateral fixtures*, a new class of fixtures for sheet-metal parts with holes. These fixtures use cylindrical jaws with conical grooves that facilitate part alignment; each jaw provides the equivalent of four point contacts. The fixtures are unilateral in the sense that their actuating mechanisms are restricted to one side/surface of the part, facilitating access to the other side/surface for assembly or inspection. We present a two-phase algorithm for computing unilateral fixtures. Phase I is a geometric algorithm that assumes the part is rigid and applies two-dimensional (2-D) and three-dimensional (3-D) kinematic analysis of form closure to identify all candidate locations for pairs of primary jaws. We prove three new grasp properties for 2-D and 3-D grips at concave vertices and define a scale-invariant quality metric based on the sensitivity of part orientation to infinitesimal relaxation of jaw position. Phase II uses a finite element method to compute part deformation and to arrange secondary contacts at part edges and interior surfaces. For a given sheet-metal part, given as a 2-D surface embedded in 3-D with e edges, n concavities and m mesh nodes, Phase I takes $O(e + n^{4/3} \log^{1/3} n + g \log g)$ time to compute a list of g pairs of primary jaws ranked by quality. Phase II computes the location of r secondary contacts in $O(grm^3)$ time.

Note to Practitioners—This paper was motivated by the problem of holding sheet-metal parts for automobile bodies but it also applies to other sheet-metal components that have cut or stamped holes. Existing approaches to fixturing such parts generally have contacting mechanisms on both sides of the sheet that restrict access for welding or inspection. This paper suggests a new approach using pairs of grooved cylinders, activated from only one side of the part (hence “unilateral”). These cylinders mate with opposing corners of holes in the sheet and push apart to hold the sheet in tension, thus acting as both locators and clamps. In this paper, we mathematically characterize the mechanics and conditions for a unilateral fixture to hold a given part. We then show how such fixtures can be efficiently computed; this can allow a computer-aided design (CAD) system (with finite element capability) to automatically generate and propose unilateral fixtures for a given part. Preliminary physical experiments suggest that this approach is feasible but it has not yet been incorporated into a CAD system nor

tested in production. In future research, we will address the design of unilateral fixtures that hold two or more parts simultaneously for welding.

Index Terms—Assembly, fixturing, form closure, grasping, modular fixturing, sheet metal, welding, workholding.

I. INTRODUCTION

SHEET-METAL parts are created by stamping and bending, and often contain holes that can be used for holding. To assemble industrial parts such as automotive bodies and large appliances, sheet-metal parts need to be accurately located and held in place by fixtures to permit assembly, welding, or inspection. Existing sheet-metal fixtures are generally bulky (limiting access to the part), nonmodular (requiring dedicated material and storage), and designed by human intuition (often resulting in suboptimal designs).

We propose *unilateral fixtures*, a new class of fixtures for sheet-metal parts with holes. These fixtures use cylindrical jaws with conical grooves that facilitate part alignment; each jaw provides the equivalent of four point contacts. The fixtures are unilateral in the sense that their actuating mechanisms are restricted to one side/surface of the part, facilitating access to the other side/surface for assembly or inspection. In contrast, conventional (bilateral) fixtures are actuated by mechanisms that approach the part from both sides a bilateral fixture consists of complex and/or bulky holding elements and mechanisms on either side of the sheet-metal part and can limit access. Fig. 1 illustrates an example.

We present a two-phase algorithm for computing unilateral fixtures. Phase I is a geometric algorithm that assumes the part is rigid and locates pairs of primary jaws at part hole concavities. For every pair of concavities, we apply a set of sufficient conditions to test the part for immobility. We prove that a rigid three-dimensional (3-D) part can be immobilized by jaws at these concavities if its two-dimensional (2-D) projections onto two orthogonal planes containing both concavities are immobilized by the projections of the jaws and if the conical grooves of the jaws prevent rotation about an axis through both concavities.

In Phase II, we consider applied forces and compute part deformations using a finite element method (FEM). We add secondary contacts at the mesh nodes that maximally restrict local part displacement. We iterate, adding secondary contacts until we find a contact set that satisfies the tolerance requirements or until no more contacts can be added.

Unilateral fixtures align the part into the desired orientation as the primary jaws are engaged. We develop a scale-invariant quality measure and show that it is consistent with a physical experiment measuring part angular displacement as the distance between primary jaws is relaxed.

Manuscript received December 18, 2002; revised January 5, 2004. This work was supported in part by the Ford Motor Company and in part by the National Science Foundation under Award DMI-0010069. This paper was recommended for publication by Associate Editor M. Wang and Editor I. Walker upon evaluation of the reviewers' comments.

K. Gopalakrishnan and K. Goldberg are with the Department of Industrial Engineering and Operations Research, University of California at Berkeley, Berkeley, CA 94720 USA (e-mail: gopal@ford.ieor.berkeley.edu; goldberg@ieor.berkeley.edu).

G. M. Bone is with the Department of Mechanical Engineering, McMaster University, Hamilton, ON L8S 4L7, Canada (e-mail: gary@mcmaster.ca).

M. J. Zaluzec is with the Ford GT Advanced Manufacturing, Manufacturing and Vehicle Design Research Laboratory, Ford Motor Company, Dearborn, MI 48121 USA (e-mail: mzaluzec@ford.com).

R. Koganti, and P. A. Deneszcuk are with the Ford Motor Company, Dearborn, MI 48121 USA (e-mail: rkoganti@ford.com; pdeneszc@ford.com).

R. Pearson is with the National Center for Manufacturing Sciences (NCMS), Ann Arbor, MI 48108 USA (e-mail: RichardP@ncms.org).

Digital Object Identifier 10.1109/TASE.2004.835572

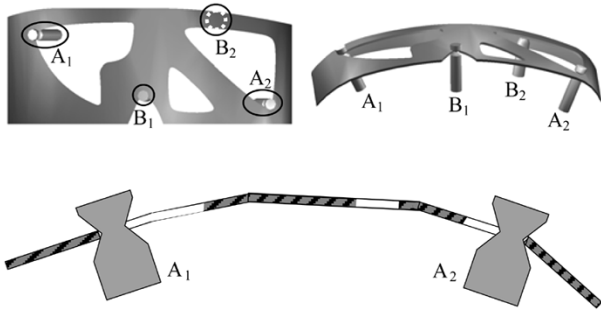


Fig. 1. Three views of an example sheet-metal part with unilateral fixture. Primary jaws A_1 and A_2 are cylindrical with conical grooves that expand between pairs of part hole concavities. These are combined with secondary jaws B_1 and B_2 . The lower figure illustrates a sectional side view (not to scale). The actuating mechanism (not shown) is below the part.

II. RELATED WORK

Workholding, grasping, and fixturing seek arrangements of contacts that restrict the possible motions of a given part. Bicchi and Kumar [2] and Mason [18] provide concise surveys of research on robot grasping. Rong and Zhu [29] provide a review of fixture design principles, modular fixturing and computer-aided fixture design.

Grasps can be classified as force or form closure. Form closure occurs when any neighboring configuration of the part results in collision with an obstacle. Force closure occurs if any external wrench can be resisted by applying suitable forces at the contacts [18], [26]. Gripper contacts can be modeled as frictional points, frictionless points or soft contacts [31]. Reuleaux [25] and Somoff [35] prove that four and seven frictionless point contacts are necessary to establish form closure in the plane and in 3-D, respectively, and [20] and [17] proved that four and seven point contacts suffice.

Rimon and Burdick [26], [27] were the first to identify and introduce the notion of second-order force closure. Immobility is defined to occur if any trajectory results in the decrease of distance between the part and at least one obstacle it is in contact with. First and second orders of immobility arise due to the truncation of the Taylor expansions of the distances at the first and second-order terms, respectively. They show that generic planar parts can be immobilized (second order) with three frictionless contacts if they are placed with infinite precision. Ponce *et al.* [23] give an algorithm to compute such configurations. Their analysis is carried out in C space $C = \mathfrak{R}^n \times SO(n)$ for an n -dimensional part. The translational degrees of freedom of the part are represented in \mathfrak{R}^n and the rotational degrees of freedom are represented by the space of rotations $SO(n)$. $SO(2)$ and $SO(3)$ are parameterized by \mathfrak{R}^1 and \mathfrak{R}^3 , respectively. Any configuration of the part in n -dimensional space is represented as a point in C space.

Rimon and Blake [28] give a method to find *caging grasps*, configurations of jaws that constrain parts in a bounded region of C space such that actuating the gripper results in a unique final configuration. They consider the opening parameter of the jaws as a function of their positions and use stratified Morse theory to find caging grasps. In this paper, we look at the distance between the jaws and use the fact that it is at a strict local extremum to show that the part is immobilized.

Plut and Bone [21], [22] proposed inside-out and outside-in grips using two or more frictionless point contacts at linear or curved part edges. They show how to find such grips where the distance between contacts is at an extremum. They achieve form closure in 3-D using horizontal V-shaped circumferential grooves (VCGs). Our unilateral model minimizes fixture profile on one part exterior and generalizes their analysis with an exact test for 3-D form closure, a new quality metric, and a method for locating secondary contacts based on FEM. Cheong *et al.* [8] give fast algorithms that generate first-order form-closure grasps of 2-D polygonal parts using two or three contacts. They find sets of contact wrenches in wrench space whose convex hull contains the origin, using a triangle search structure. This algorithm is used to increase the speed of Phase I of our two-phase algorithm.

In fixturing, Hurtado and Melkote [12] study how a fixture's conformability and stability vary with design parameters such as number and positions of contacts and geometric properties of the fixture elements. They develop two metrics based on global and local conformability (based on similarity of shape between the part and the circumscribing polyhedron fitting the contacts). By minimizing the net complementary energy of the fixture and part system, the reactionary forces were evaluated at the contacts and used to observe trends of conformability and stability as the design parameters varied. Johannesson and Soderberg [13] analyze tolerance chains and tolerance sensitivities by modeling geometric variations in a tree structure. Every coupling constraint is modeled in the tree. Parts of the tree are extracted for analysis depending on the area of interest. The robustness of the assembly is also evaluated using Monte Carlo simulations. Wang [39] examines the errors in machined features in relation to the errors in locator position and locator surface geometric errors. The relation is expressed using a critical configuration matrix for the part. Wang suggests an optimal locator configuration based on the error sensitivity of multiple part features. Xiong *et al.* [40] develop a statistical model for analysis of geometric variations in assemblies. They model the stacking of incremental errors in each assembly station, and based on locator errors and geometric errors of individual parts, determine the error in position or orientation of the feature being analyzed. The predicted errors are used to study assembly methods and sequences to choose an optimal assembly process. Carlson and Soderberg [7] perform a root-cause analysis of dimensional errors in an assembly. They study the degrees of freedom of each feature and each locator and track assembly variations into the variations at each locator. They also derive conditions guaranteeing diagnosability of a dimensional error by modeling variations as a linear program.

Wagner [37] proposes a method to fixture rigid 3-D polyhedra using struts normal to each surface. He proves that first-order form closure of the polyhedron is equivalent to first-order form closure of each of the three projections of the part and the contacts on to the three orthogonal planes. An efficient geometric algorithm to compute all placements of four frictionless point contacts on a polygonal part that ensure form closure is described by van der Stappen *et al.* [36]. Given a set of four edges, they show how to compute critical contact placements in constant time. The time complexity of their algorithm is bounded by the

number of such sets. For the specialized case of v -grips, their algorithm runs in an expected time of $O(n^2 \log n)$ for n vertices.

Recent progress on fixturing deformable and sheet-metal parts builds on the work of Menassa and De Vries [19] who determine the positions of datum points needed to locate the part in the correct plane for 3-2-1 fixturing. They use an FEM of the part to model the deformation, and determine fixture locations by optimizing an objective that is a function of the deformations at the mesh nodes. Our Phase II is modeled on their approach, which is extended by [5] and [24]. Rearick *et al.* [24] design a fixture for a sheet-metal part by using an objective function that is a weighted sum of the norm of the deformation and the number of fixtures in the objective function. They use a remeshing algorithm, but do not address properties specific to sheet-metal parts such as buckling. Cai *et al.* describe an N-2-1 fixturing principle in [5]. This is used instead of the conventional 3-2-1 principle to reduce deformation of sheet-metal parts. They use $N(\geq 3)$ locators for the primary datum, (i.e., they use N datum points to locate the sheet-metal part in the correct plane) in their fixtures. They model the sheet-metal parts using finite elements with quadratic interpolation, constraining mesh nodes in contact with the primary datum to only in-plane motion. For a known force, linear static models are used to predict deformation. To make their algorithm faster, instead of remeshing the part for different locator positions, they express the constrained displacement at the locator by using a linear interpolation of displacement at the adjacent nodes. Fixture elements are placed such that compressive forces that cause buckling do not occur. In contrast, our two-phase approach is a hybrid of geometric and FEM methods.

Wang [38] and Ding *et al.* [9] study using discretized domains of fixture element locations to create fixtures. Wang [38] describes an algorithm to obtain an optimal fixture for a domain of discrete contacts with six locators and one clamp. The optimality is obtained by considering localization accuracy and force balance at the contacts. Ding *et al.* [9] proposes a method for fixture design for curved workpieces by discretizing the part's surface to obtain contact locations. They start with a random set of contacts and randomly iterate contact locations till form closure is achieved. The number of iterations is reduced by eliminating sets of contacts based on a facet that divides the domain of contacts into two parts based on the property that the contact wrenches need to positively span the wrench space. Only half-space defined by the facet is considered. Li *et al.* [15] describe a procedure to design fixtures for two sheet-metal parts that are to be welded to produce a good fit along the seam to be welded. The fixtures are designed using an FEM to determine either an optimal fixture or a robust fixture. Li *et al.* [16] describe a dexterous part holding mechanism based on vacuum cups and model the elastic deformation of the sheet-metal part using FEMs and a statistical data model. The results from this model are used to minimize the part's deformation. Shiu *et al.* [33], [34] give a heuristic algorithm to analyze the deformation of a sheet-metal part by decoupling it into beams based on the part's features. Based on the deformations predicted, they give an algorithm to allocate tolerances to each feature.

Asada and By [1] describe a reconfigurable fixturing system and study the kinematics of the part in contact with fixture ele-

ments in the workspace. They derive conditions for uniquely locating a part in a fixture and for immobility. For modular fixtures, Brost and Goldberg [4] present the first complete synthesizing algorithm that guarantees to find a fixture, consisting of three locators and one clamp if one exists. They enumerate all such fixtures by choosing candidate fixture element positions that are at a distance permitted by the edges of the part the elements are in contact with. Rong and Li [30] present an interactive rapid fixture design system (RFDS) that allows a designer to make use of several databases of fixture components, location method, etc. and automates the generation of a modular fixture subject to the specifications of the user regarding positions and orientations of the components. Sela *et al.* [32] consider the fixturing of a sheet-metal workpiece using clamps and locators fixed on a base-plate with t-slots. The height of the fixture elements are variable, and are adjusted to fit the shape of the part. They determine the positions of the locators and clamps by formulating a nonlinear programming problem in terms of the part deformation. Li *et al.* [14] design fixtures for laser welding by first identifying a robust design space where the sensitivity of part deformations to part dimension and jaw location errors. Within this space, they use a genetic algorithm to find a fixture that minimizes an objective function defined in terms of the distance between the weld joint nodes of each weld stitch.

Unilateral fixtures are modular and combine simple hardware with rigorous algorithmic analysis [6]. This paper is a greatly revised and extended version of ideas initially reported in [10] and [11].

III. PROBLEM STATEMENT

The input is a model of a part sheet-metal part: a contiguous connected 2-D surface embedded in 3-D with holes whose thickness is assumed to be small compared to the dimensions of the features on the part. It is defined by a computer-aided design (CAD) model that consists of a list of its edges: both external and internal (holes) in terms of spline curves, and a list of Bezier surfaces that define the part surface. For each edge, the side of the edge on which the part lies is also specified. The desired orientation of the part is specified by defining the CAD model using a coordinate frame where the desired baseplate lies in the x - y plane. An FEM mesh discretizing the part is also specified as a triangular or quadrilateral mesh (but other meshes can be used), and the part thickness is specified for each mesh element. Other inputs are specified below.

As illustrated in Fig. 1, primary jaws consist of two coaxial frustums of cones joined at their narrow ends which have equal radii (called the radius of the jaw). Secondary contacts may either be of the same shape as primary jaws, or may be surface contacts that support the interior of the part. We assume that contacts are rigid and frictionless and do not interfere with each other when placed at mesh nodes. The frictionless assumption is conservative in the sense that a fixture that holds a part in the absence of friction will hold the part when friction is present too. However, friction can cause jamming during part loading, which is a subject for future research.

Contacts cannot be placed in specified *stay-out* regions where manufacturing equipment may need to access the part. For ex-

ample, regions around welding spots may need to be left clear for access by welding guns. If contacts need to be confined to a *stay-in* region, the complement of the stay-in region is specified as a stay-out region. Stay-in regions may include high precision features that facilitate precise location of the part when it is fixtured. Stay-in and stay-out regions are specified as lists of mesh nodes. The part is subjected to a set of known external wrenches specified as a list describing each wrench vector and the mesh node where it is applied. Tolerance δ is specified as the magnitude of the maximum deformation of any mesh node from its nominal position.

Input: This consists of a CAD model of part with FEM mesh (as specified above), Young's modulus and Poisson's ratio for the part, jaw radii, stay-out regions, list of applied wrenches at nodes, and tolerance δ .

Output: This consists of a unilateral fixture that holds the part within the given tolerance or a report that no solution exists.

In Section IV, we establish preliminary results regarding fixturing 2-D and 3-D parts with primary contacts using two jaws. We also present scale-invariant quality metrics to evaluate pairs of primary jaw locations.

IV. PHASE I: COMPUTING PRIMARY CONTACT PAIRS

A. Kinematic Analysis: 2-D V-Grips

1) *Two-Dimensional V-Grip Definition:* In order to establish fast sufficient conditions for immobility in Phase I of our algorithm for computing 3-D unilateral fixtures, we develop kinematic results on immobility of 2-D parts. We give necessary and sufficient conditions for immobilizing a 2-D part with two jaws. These conditions will be repeatedly called with projections of the 3-D sheet-metal part onto pairs of orthogonal planes.

Let v_a and v_b be two concave vertices. The unordered pair $\langle v_a, v_b \rangle$ is an expanding or contracting *v-grip* if jaws placed at these vertices will provide frictionless form closure of the part. A *v-grip* is *expanding* if the jaws move away from each other and *contracting* if the jaws move toward each other to make contact with the part.

Given jaw radius and the vertices of polygons representing the part boundary and holes in counter-clockwise order, we can compute a list (possibly empty) of all *v-grips* and sort this by a quality measure defined below.

2) *Test for Form Closure:* The key to this subprocedure is a constant-time test for form closure. We consider a pair of concave vertices $\langle v_a, v_b \rangle$. Let v_{x-1} and v_{x+1} be the vertices adjacent to v_x . Let \mathbf{u}_{x-1} be the unit vector from v_x to v_{x-1} , and \mathbf{u}_{x+1} the unit vector from v_x to v_{x+1} . Let \mathbf{u}_{xy} be the unit vector from v_x to v_y .

We construct normals at v_a , to both edges bordering v_a . This splits the plane into four regions (see Fig. 2). We number these I to IV. We do a similar construction with v_b .

Theorem 1: $\langle v_a, v_b \rangle$ is an *expanding v-grip* if and only if v_a lies strictly in region I of vertex v_b , and v_b lies strictly in region I of vertex v_a .

Theorem 2: $\langle v_a, v_b \rangle$ is a *contracting v-grip* if and only if either

- a) v_a lies in region IV of vertex v_b , and v_b lies in region IV of vertex v_a , at least one of them strictly;

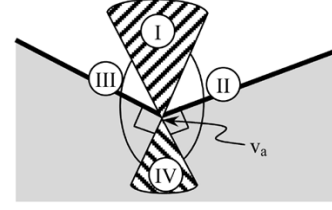


Fig. 2. Two normals at a concave vertex partition the plane into four regions that define *v-grips*.

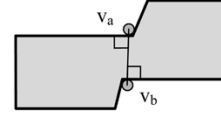


Fig. 3. Typical example of *v-grips* where the second condition in Theorem 2 holds.

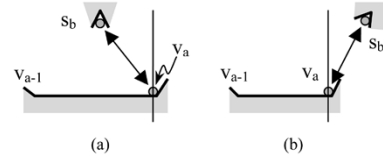


Fig. 4. $s_b v_a$ is (a) a strict local maximum or (b) a local minimum for s_a in $v_{a-1} v_a$.

- b) $\mathbf{u}_x \cdot \mathbf{u}_y = -1$ and $\mathbf{u}_x \cdot \mathbf{u}_{ab} = \mathbf{u}_y \cdot \mathbf{u}_{ab} = 0$ for at least one set of values of $(x, y) = (a \pm 1, b \pm 1)$, and the jaws approach from outside the region between the parallel lines (see Fig. 3).

3) *Proof of Theorem 1:* Let P represent part perimeter parameterized by arclength s . Let s_a and s_b represent the positions of the jaws on P . Following [3] and [28], we express the distance between the jaws as $\sigma : P \times P \rightarrow \mathbb{R}$, a function of (s_a, s_b) . The $\sigma(s_a, s_b)$ surface is positive except when it touches the plane along the diagonal $s_a = s_b$ (where it is 0), as these points represent coincident jaws. The s_a - s_b plane can be partitioned into rectangles whose sides are equal in length to the sides of the polygon. In each of these regions, the distance function is defined by a quadratic expression.

To prove Theorem 1, we prove that the following four statements are equivalent.

- A) v_a and v_b are concave and they each lie in the other's region I.
- B) $\sigma(s_a, v_b)$ is a strict local maximum at $s_a = v_a$, and $\sigma(v_a, s_b)$ is a strict local maximum at $s_b = v_b$.
- C) $\sigma(s_a, s_b)$ is a strict local maximum at $s_a = v_a$ and $s_b = v_b$.
- D) $\langle v_a, v_b \rangle$ is an expanding *v-grip* for the part.

$B \Leftrightarrow A$: This is clearly seen since the shortest distance from a point to a line is along the normal to the line (Fig. 4).

$C \Rightarrow B$ follows from the definitions.

$B \Rightarrow C$: Assume B. Since $B \Leftrightarrow A$, A is true.

Therefore, v_b lies strictly in region I of v_a . Hence, there exists a small region, say a circle of radius ε (a small length) around v_b , which also lies completely in region I (Fig. 5).

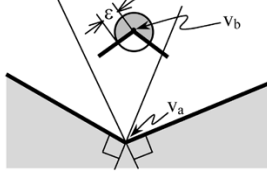


Fig. 5. $\sigma(v_a, s_b)$ is a local maximum of $\sigma(s_a, s_b)$ for any s_b in the neighborhood of v_b .

Consider any v'_a in P , within ε from v_a , and v'_b in P within ε from v_b . Since v_a is in v_b 's region I, $\sigma(v_a, s_b)$ is a local maximum at $s_b = v_b$. Therefore, $v_a v_b > v_a v'_b$. Since v'_b also lies in v_a 's region I, $v_a v'_b > v'_a v'_b$. Thus, $v_a v_b > v'_a v'_b$. Therefore, $C \Leftrightarrow B$.

$C \Rightarrow D$: Assume that C is true and D is false. Since $A \Leftrightarrow C$, A is true. Since $\sigma(v_a, v_b)$ is a local maximum and D is false, the part is not held in immobility. Since immobility is defined to occur when no neighboring point in C-space is collision-free, this means that there exists a neighboring point in C-space that does not result in collision. In other words, the part can be displaced infinitesimally. Since C is true, at least one jaw must break contact with the part in the new configuration.

If both jaws break contact, we can move the part along the directions $\pm \mathbf{u}_{ab}$ till contact occurs as both vertices are concave and hence have an angle of less than 180° from the direction of the jaws' approach. As a result, movement in at least one of two opposite directions results in contact. From this position, we can slide the part along the contact edge moving the vertex toward the jaw, till contact occurs with the other jaw or till the vertex is at the jaw. Since $v_a v_b$ is a strict maximum, the vertex has to be reached. However, since A is true, \mathbf{u}_{ab} is at acute angles to \mathbf{u}_{a-1} and \mathbf{u}_{a+1} , and \mathbf{u}_{ba} is at acute angles to \mathbf{u}_{b-1} and \mathbf{u}_{b+1} . Therefore, when the vertex reaches the jaw, the other jaw would collide with the interior of the part: thus the part cannot move and is in form closure. See Fig. 6.

$D \Rightarrow C$: Assume D is true and C is false. Then, $\sigma(v_a, v_b)$ is not a local maximum. Either it is a strict local minimum or it is not a strict local extremum. If $v_a v_b$ is a strict local minimum it can be shown that $\langle v_a, v_b \rangle$ is a contracting v -grip, and hence, D cannot be true. If $v_a v_b$ is not a strict extremum, then by the continuity of s , the part can move along the contour $\{(s1, s2) \mid \sigma(s1, s2) = \sigma(v_a, v_b)\}$. This contradicts D. Therefore, C is true.

Thus, $D \Leftrightarrow C$, completing the proof for theorem 1. We can prove Theorem 2 similarly. The second condition in Theorem 2 arises due to the limiting case where vertex lies on the boundary of region IV.

Corollary 1: If the second condition in Theorem 2 is ignored, and all the inequalities are made strict inequalities in theorem 2, theorems 1 and 2 give necessary and sufficient conditions for first-order immobility.

This can be proved from 1) first-order form closure, which is a subset of immobility, and 2) center of rotation analysis. For the center of rotation analysis, all the configurations excluded by making the conditions in Theorem 2 stricter can be seen to be second-order immobility as they give rise to coincident normals that cannot cause first-order immobility, but cause immobility. Also, the remaining configurations are first order because the

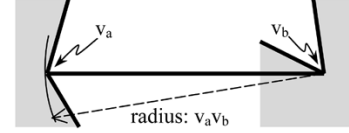


Fig. 6. Edges are at acute angles to $v_a v_b$.

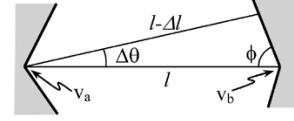


Fig. 7. Deriving an expression for $|d\theta/dl|$.

normals cannot coincide and cannot be concurrent (as two of the four points of intersection are at distinct vertices), and all centers of rotation are excluded as we know the part is immobile.

Corollary 2: For a nonpoint jaw with a convex shape, the v -grips can be generated by applying the theorems to a transformed part generated by doing a Minkowski sum of part shape with jaw shape.

This can be seen as the transformed part gives the locations of the jaws' center that result in collision with the part, and thus also the shape of the cross sections of the C -obstacles. The curved edges generated by doing the sum can be ignored as they correspond to undesirable contacts with convex vertices of the part.

4) *2-D Quality Metric:* We can compare v -grips based on how much the part can rotate when the jaws are relaxed infinitesimally. We define a scale-invariant measure of the sensitivity of the grip to such infinitesimal disturbances. Given a v -grip $\langle v_a, v_b \rangle$, let $l = \sigma(v_a, v_b)$. If the distance between the jaws changes by Δl , let $\Delta \theta$ be the maximum angle the part can rotate. Clearly, $\Delta \theta$ depends on Δl . We consider the ratio $\Delta \theta / (\Delta l / D)$, where D is the diameter of the part (the maximum distance between any two points on the part). For infinitesimal Δl , this becomes $D(d\theta/dl)$. We rank pairs of primary jaws based on $|D(d\theta/dl)|$: smaller ratios correspond to smaller errors.

The maximum error in orientation occurs when one jaw is at a concave vertex and one jaw is on an edge. To derive an expression for $|d\theta/dl|$, we consider one edge at an angle ϕ to $v_a v_b$. Using the sine rule applied to the triangle shown in Fig. 7

$$\frac{(l - \Delta l)}{(\sin \phi)} = \frac{l}{(\sin(\phi + \Delta \theta))}.$$

If we neglect second-order terms, this simplifies to

$$\left| \frac{d\theta}{dl} \right| = \lim_{\Delta l \rightarrow 0} \left| \frac{\Delta \theta}{\Delta l} \right| = \left| \frac{\tan(\phi)}{l} \right|.$$

For all four edges, we choose the one with ϕ closest to 90° , which yields the maximum possible change in orientation. For this value of ϕ , the metric will be $|D \tan(\phi)/l|$. This quality metric is dependant on the local geometry of the part and is scale-invariant since the distance between the jaws scales with the diameter of the part. As a result, the first-order error in part position is invariant to part diameter.

B. Kinematic Analysis: 3-D VG-Grips

1) *Three-Dimensional VG-Grip Definition:* We use two orthogonal 2-D projections to analyze 3-D parts. The primary jaws are designed to engage the 3-D part at its concavities such that the intersections of the frustums in the jaws are seated in the plane of the sheet-metal part. For the part to contact the jaws on the plane of intersection of its frustums, the local radius of curvature of the part needs to be large compared to the jaws' radius. If this is not true, contact does not occur on the plane, but instead, on the surfaces of the individual cones. Therefore, at such candidate jaw locations, we assume local planarity of the part and linearity of the edges for first-order analysis of immobility, since only local shape is of importance. We construct tangents at the points of contact. We call these tangents the part's "virtual edges," and the point of intersection of the edges, the corresponding "virtual vertex." If we approximate the part locally using the virtual edges and vertices, immobility of the approximation will be equivalent to the immobility of the original part up to the first order. The jaws' positions are described in terms of the virtual vertices. Virtual vertices are concave by definition. Given two virtual vertices v_a and v_b , we call the unordered pair $\langle v_a, v_b \rangle$ a 3-D *vg-grip* if the part is held in form closure when the jaws' grooves engage the part at the edges defining v_a and v_b .

Given jaw radius and the 3-D CAD model of the part, we can compute a list (possibly empty) of all *vg-grips* and sort this by a quality measure defined below. We can also compute bounds on jaw cone angles for each *vg-grip* found.

2) *Candidate Jaw Locations for the 3-D Part:* As stated above, while contact occurs near vertices for a part defined by linear edges, parts with curved edges have virtual vertices near which the jaws engage the part. Each virtual vertex corresponds to a unique candidate jaw location where a jaw may be located to engaging the part at the virtual edges corresponding to the vertex. Candidate jaw locations and corresponding virtual vertices are identified using the following subprocedure, which uses the fact that jaws contact the part at two points only if there is a concave vertex between the points of contact or if part of the edge contained between the points of contact is concave and has higher curvature than the jaw.

- Step 1) Set list L as list of the part's concave vertices. Set list L_c to an empty list.
- Step 2) Traverse each edge of the part. For each edge, numerically identify concave stretches with radius of curvature less than jaw radius, and add the end points (with greater arc-length) to L .
- Step 3) For each point i in L , traverse the edge starting from the point i in the direction of increasing arc-length, constructing discs tangential to the edge on the tangent plane of the surface at the point considered till the disc touches the part at two points or the entire edge is traversed back up to the position of the current element of L .

If the entire edge was not traversed and if the edge at the second point of contact is in plane with the disc, and the principal radius curvature of the surface at both points of contact is larger than the

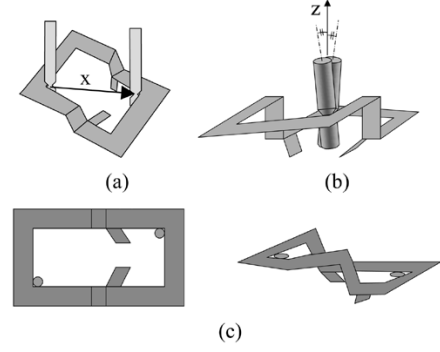


Fig. 8. (a) x axis is chosen along the line connecting the vertices v_a and v_b . (b) In a projection perpendicular to the x axis, the z axis is chosen as the bisector of the acute angle between the jaws' axes' projections. (c) 2-D *v-grips* in two orthogonal projections.

radius of the disc, and the disc does not lie in a stay-out region, add the center to L_c . Replace the current element of L by the point of intersection of the tangents.

Else, delete the current element of L .

- Step 4) Traverse L_c for duplicates and eliminate them and the corresponding elements in L .
- Step 5) Return the list L as the list of candidate locations and L_c as the list of centers.

3) *Sufficient Test:* As shown in Fig. 8, we define a coordinate system such that the direction of the x axis is taken from v_a to v_b . In a projection perpendicular to the x axis, the z axis is defined as the bisector of the acute angle between the projections of jaw axes. When jaw axes projections are parallel, the z axis is defined at 45° to the jaws' axes. The y axis is perpendicular to the x and z axes using the right-hand rule. Let the points of contact have position vectors \mathbf{r}_{a1} , \mathbf{r}_{a2} , \mathbf{r}_{b1} and \mathbf{r}_{b2} . Let the vectors \mathbf{a}_a and \mathbf{a}_b be the axes of the jaws with positive z components and the centers of the intersections of the cones be c_a and c_b . (The subscripts a and b denote the jaws at vertices v_a and v_b .) We define \mathbf{q}_{a1} as $\mathbf{e}_x \times ((\mathbf{r}_{a1} - \mathbf{v}_a) - (\mathbf{r}_{a1} - \mathbf{v}_a \cdot \mathbf{e}_x)\mathbf{e}_x) = \mathbf{e}_x \times (\mathbf{r}_{a1} - \mathbf{v}_a)$, and similarly \mathbf{q}_{b1} , \mathbf{q}_{a2} , and \mathbf{q}_{b2} .

Theorem 3: Assuming that the part is rigid, immobility is achieved if all of the following are satisfied.

- a) The projection of the part and jaws on the x - y plane is a 2-D *v-grip*.
- b) The projection of the part and jaws on the x - z plane is a 2-D *v-grip* of the same nature (expanding or contracting).
- c) At least one of the eight angles between \mathbf{q}_{xi} and the inward normal to the cones at \mathbf{r}_{xi} (for $x = a, b; i = 1, 2$) is less than 90° , and at least one of the angles between $-\mathbf{q}_{xi}$ and one of the inward normals at \mathbf{r}_{xi} is less than 90° .

4) *Proof of Theorem 3:* The distance between the jaws is defined as the x component of the distance between the centers of the cones' intersections. We will show that any small displacement of the part requires a decrease in distance between the jaws if one jaw is fixed and the other is allowed to translate. Hence, since the jaws are fixed, the part will be in form closure.

Consider any small displacement of the part. This can be denoted as the sum of three translations and three rotations (along

and about the x , y and z axes). We show that as the part is subject to each of these components of displacement while keeping the distance between them at the local maximum of the possible distances, the distance between them decreases.

From condition c) in Theorem 3, any rotation of the part about the x axis should result in a decrease of distance between the jaws. This is because the vectors \mathbf{q}_{xi} , $x = a, b$; $i = 1, 2$, give the direction of the instantaneous velocities of each contact. Hence, if a jaw stays in the same position, it collides with the part, i.e., it has to move either toward or away from the vertex. It cannot move toward the vertex because of the following reason: If we scale down the part and the jaw about the vertex, such that the distance between the scaled jaw and the vertex is equal to the distance between the vertex and the jaw after the rotation, the scaled jaw would collide with the part after an identical rotation (since the conditions are scale-independent). Since a smaller jaw would collide with the part in such a position, the original bigger jaw will also collide with the part, since the vertex and edges of the part do not change on scaling. Hence, each jaw is pushed away from the vertex.

First-order form closure is robust in the sense that immobility is guaranteed allowing for small changes in part geometry. Since none of the axes are perpendicular to the planes of intersections of each jaw's cones, conditions a) and b) of Theorem 3 ensure that the projections of the part on the x - y and x - z planes are in form closure after an infinitesimal rotation of the part about the x axis. We note that the distance between the vertices does not change as a result of rotation about the x axis. Since the distance between the vertices remains the same due to such a rotation and since the edges are linear and the vertices concave, it follows from Theorem 1 that the distance between the jaws decreases.

Condition a) also implies that translation along the x or y axes, and rotation about the z axis will result in further increase in the distance between the jaws. Condition b) implies that any further translation along x or z axes and rotation about the y axis leads to another increase in distance. Thus, any displacement of the part results in a displacement of the jaws, hence proving that form closure is achieved if the jaws are fixed.

5) *Bounds on Cone Angles:* Conditions a) and b) in Theorem 3 are independent of the cone shapes for a given jaw radius. Hence, bounds on the cone angles that satisfy Theorem 3 are determined only by condition c). In the worst case, $\pm\mathbf{q}_{xi}$, $x = a, b$, are tangential to the cones for at least 1 value of $i = 1, 2$. Hence, if we project $\pm\mathbf{q}_{xi}$ to the plane containing \mathbf{r}_{xi} and \mathbf{a}_x , the acute angles between the projections and $\pm\mathbf{a}_x$ give a candidate lower bound for the half cone angle for the upper cone. For instance, the lower bound is chosen as the higher of candidate bounds obtained from \mathbf{q}_{x1} and \mathbf{q}_{x2} . For the 3-D sheet-metal part example shown in Fig. 1, the bounds for the half cone angles for the four cones were 18° , 21° , 18° , and 26° .

6) *3-D Quality Metric:* We generalize our scale-invariant quality metric to 3-D parts: it is the maximum change in orientation along any of the coordinate axes due to an infinitesimal relaxation of the jaws, $|D(d\theta/dl)|$, l being the distance between the jaws, and θ the orientation. Based on the above sufficient test, for the y and z components of orientation, this reduces to the metric defined for 2-D. For rotation about the x axis, this is

not the case. We find an approximate value for $|D(d\theta/dl)|$ by assuming that the contacts lie on the vertices of the v -groove in the projection of the jaws on a plane perpendicular the plane containing the contacts and the edges. Since the contacts on the jaw projection hold the jaw in a v -grip, we know that distance between the contacts increases by $q_a\Delta\theta$, where q_a is the quality metric for this v -grip. Hence, if the original distance between the centers of jaw a and the vertex is d_a , the distance after rotation is $d_a(1+q_a\Delta\theta/|\mathbf{r}_{a1}-\mathbf{r}_{a2}|)$. Thus, the metric for rotation about the x axis simplifies to $D(|\mathbf{r}_{a1}-\mathbf{r}_{a2}|/d_a q_a + |\mathbf{r}_{b1}-\mathbf{r}_{b2}|/d_b q_b)$. The quality of the vg -grip is the maximum of the metrics for all three rotations, which is scale invariant.

V. PHASE II: COMPUTING SECONDARY CONTACTS

Phase I assumes the part is rigid and computes a list of pairs of jaws that immobilize the part. Phase II considers each pair and adds secondary contacts (if necessary) using an FEM deformation model. Secondary contacts are of two types: 1) edge contacts that are shaped similar to primary jaws (cylindrical with conical grooves) and engage the part at its edges and 2) surface contacts that are cylindrical with rounded tips that provide point contacts on part surfaces.

We model part deformation we use FEM, based on the given mesh. Forces or wrenches specified at each mesh node (as part of the input to the problem) are included as force boundary conditions in the FEM model. Displacement boundary conditions are generated by the contacts. Edge contacts constrain the point of contact to lie on the tangent to the edge, and surface contacts constrain the point of contact to lie on the tangent plane to the surface at the point of contact. The FEM model gives the deformation as a vector of the displacements of each mesh node.

We consider the list of primary contact pairs generated by Phase I. We use the deformation model to determine the displacements of each node. For each mesh node on the part's edges, we consider the magnitude of the displacement in the plane containing the tangent to the edge and the normal to the surface at the node. The magnitude is positive if the component of displacement in the tangent plane of the part is away from the interior of the part, and negative otherwise. For each node on the part's interior, we consider the component of the displacement along the negative z axis in the frame of reference of the CAD model. We then choose the node with the highest such component of displacement from among both edge and surface nodes that do not lie in stay-out regions, and add a contact at this node. We note that due to the nature of the FEM interpolation, the maximum displacement for any point on the part lies at an FEM node. We add a contact at this node. We perform this for each pair of primary jaws generated by Phase I.

We repeat the above subprocedure to add more secondary contacts until we find a contact set that satisfies the tolerance requirements or until no more contacts can be added. Fig. 9 shows an example of adding secondary contacts during Phase II.

VI. COMPUTATIONAL COMPLEXITY

Recall that the polygonal part is described by n vertices. For the polygonal part, we find $k \leq n$ concave vertices flanked by straight edges in $O(n)$ time. We then consider each pair of

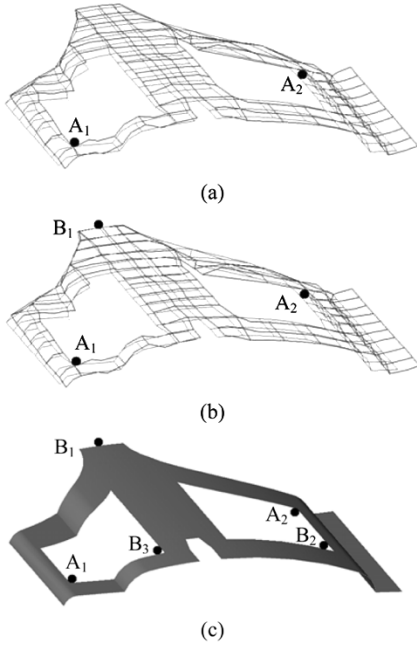


Fig. 9. (a) Deformed and (b) undeformed meshes for first two iterations of Phase II. Final fixture (c) required four iterations.

concave vertices, checking the conditions in Theorems 1 and 2 in constant time. The result is a set of up to k^2 v -grips. Thus, all v -grips are found in $O(n + k^2)$ time. Computing the quality metric takes constant time for each v -grip and sorting requires $O(k^2 \log k)$ time as there are at most k^2 v -grips.

For a sheet-metal part, given e edges and n concavities, $O(e + n)$ time is needed to determine the concavities. There are at most $O(n^2)$ pairs of candidate primary jaw locations. We can use the output-sensitive algorithm of Cheong *et al.* [8] to compute them in time $O(e + n^{4/3} \log^{1/3} n + g)$ time, where g is the number of pairs found. An additional $O(g \log g)$ time is required to sort the pairs by the quality metric.

In Phase II, running the FEM deformation analysis for the mesh of m nodes involves solving a set of $O(m)$ linear equations which requires time $O(m^3)$. To find unilateral fixtures with r contacts, Phase II runs in $O(m^3 r)$ time for each pair of primary contacts, yielding an overall runtime of $O(e + n^{4/3} \log^{1/3} n + g \log g + gm^3 r)$.

VII. IMPLEMENTATION AND EXPERIMENT

We implemented the 2-D v -grip subprocedure in Visual BASIC on a Pentium III 1.13 GHz PC running on Windows XP. For a part with 30 vertices and ten concave vertices the program execution time was under 0.0084 s. A Java implementation is available for online testing at <http://alpha.ieor.berkeley.edu/vgrip>.

For Phase II for the sheet-metal part shown in Fig. 9, we used ANSYS to perform four iterations using a quadrilateral mesh with 274 nodes in 1.3 s. For this example we used a tolerance equal to half the allowed error in relative positions of points on mating parts where spot welds occur for automotive parts as specified by the Ford Motor Company.

As illustrated in Fig. 10(b), we constructed an experimental apparatus to study how the quality metric compares with part

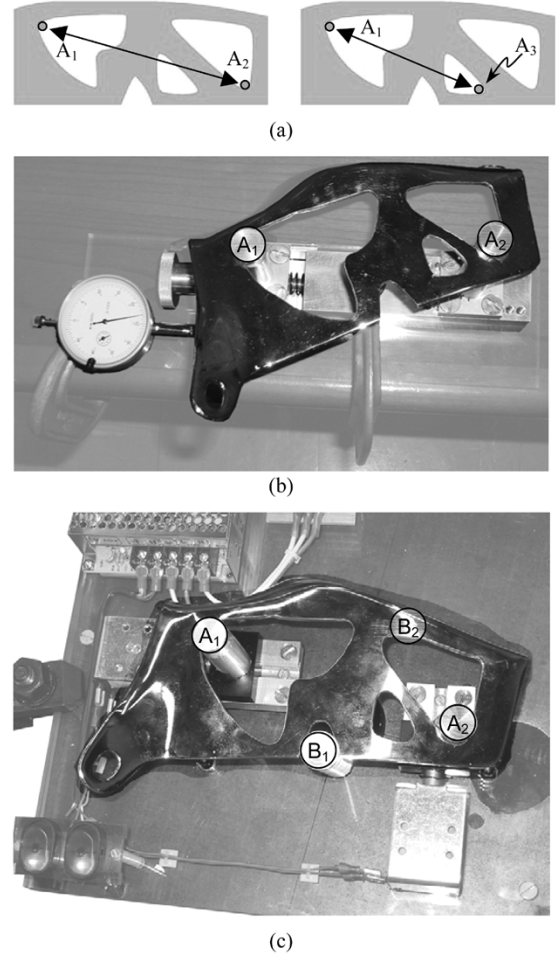


Fig. 10. Quality metrics of two vg -grips (a) were compared by physical experiments using the apparatus shown in (b). Dial gauge is used to measure the relaxation of the jaws. The error in orientation is measured by reflecting a laser on a mirror on the top-right of the part. Unilateral fixture prototype shown in (c) has two primary jaws A_1 and A_3 activated by solenoids. Secondary contacts are at B_1 and B_2 .

orientation error as the jaws are relaxed for the two vg -grips shown in Fig. 10(a). We used a chrome-plated automotive part 9.4 inches in diameter held by a pair of primary jaws. One primary jaw was fixed on the baseplate, and the other was constrained to move toward or away from the first jaw. The second jaw was manually actuated by rotating a ballscrew. A locking screw was used to fix the jaw rigidly at any position. We used a dial gauge mounted on the baseplate to measure the distance between the jaws. To accurately measure the angular orientation of the part, we mounted a mirror on the part and reflected a laser beam off the mirror onto a surface with a 1mm grid.

Initially, the part was immobilized using the pair of primary contacts. We achieved this by incrementally increasing the distance between the jaws, tightening the locking screw, and manually applying small forces on the part to test if it could be displaced. Once the part was held rigidly, we measured and recorded the distance between the jaws. We then loosened the locking screw and incrementally relaxed the jaw in steps of 0.0005 inches. At each increment, we tightened the locking screw, perturbed the part by hand, and recorded the maximum error in orientation. We reduced the distance between the jaws

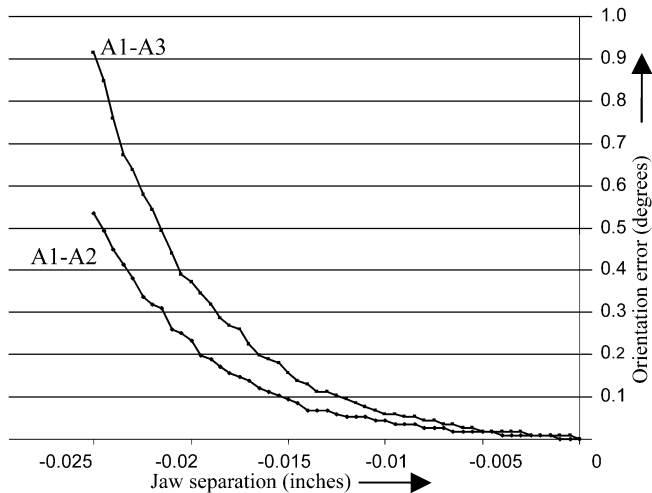


Fig. 11. Quality metric comparison. Using the apparatus shown in Fig. 10(a), part orientation error is measured as a function of jaw separation for the two primary contact pairs shown in Fig. 1. Jaw separation is zero when the jaws are fully opened. The scale-invariant quality metric is related to the slope at zero of the curve as described in Section IV-B-VI. The quality metric for pairs A_1-A_2 and A_1-A_3 are 31.74 and 77.43, respectively, indicating that the former pair has better resistance to part orientation error, as confirmed by the data.

50 times, and then increased the distance in increments of 0.0005 inches till a 3-D *vg-grip* was achieved again. This was done to check for plastic deformation of any portion of the experimental apparatus. We repeated this procedure twice to get a total of 200 readings. In Fig. 11, we plot orientation error as a function of jaw separation (relative to fully expanded position). The plot confirms that primary contact pair A_1A_3 allows more angular error than primary contact pair A_1A_2 , consistent with the quality metric.

We constructed a prototype of a unilateral fixture [Fig. 10(c)] for the same part. The fixture consists of primary jaws A_1 and A_2 , and secondary jaws B_1 and B_2 . The part is loaded on the fixture by supporting it on B_1 , B_2 and three additional contacts. Primary jaws are actuated by solenoids to move along dovetail tracks to move into position to engage the part. The additional contacts used to load the part are then removed. We measured the repeatability of part orientation when the jaws were actuated. We carried out 50 trials each for simultaneous actuations of the primary jaws and both sequences of actuating the jaws one at a time.

Actuating the jaw A_1 in 10(c) before jaw A_2 resulted in higher precision. The errors over the 150 trials ranged from -0.24° to $+0.12^\circ$ with the exception of three outliers, with a standard deviation of 0.11° . The order of actuation makes a difference due to the presence of friction in the experimental apparatus. As a result, the part can be seated on the jaws' grooves in an orientation that depends on the order of actuation.

We represent the error as the error in orientation since unlike position errors, it is independent of the reference points chosen for measurement for rigid bodies. As noted in Section IV-A-4, the first-order position error is invariant to scale for a given relaxation of the jaws. This is because the distance between the primary jaws scales with the part making the quality metric scale-invariant.

VIII. SUMMARY AND FUTURE WORK

In this paper, we proposed unilateral fixtures, a new class of fixtures for sheet-metal parts where primary holding elements are cylindrical jaws with conical grooves that expand between pairs of part hole concavities and secondary contacts are arranged to reduce part deformation. We develop new analytic results in 2-D and 3-D, new quality metrics, and specify a two-phase algorithm that analyzes part geometry to automatically compute unilateral fixtures.

In future work, we will develop a formal model of unilateral fixture loading and algorithms for placing loading contacts. We will consider the effects of friction and gravity during loading. We will also consider unilateral fixtures for pairs of mating parts. We will model the deformation of mating parts and minimize the error in the relative deformations of points where joining occurs.

ACKNOWLEDGMENT

The authors would like to thank J. Alton for design and implementation of the prototypes, R. Alterovitz, A. Levandowski, D. Song and P. Wright for their contributions, and the editors and anonymous reviewers for their detailed feedback.

REFERENCES

- [1] H. Asada and A. B. By, "Kinematics of workpart fixturing," in *Proc. IEEE Int. Conf. Robotics Automation*, vol. 2, Mar. 1985, pp. 337-345.
- [2] A. Bicchi and V. Kumar, "Robotic grasping and contact: A review," in *Proc. IEEE Int. Conf. Robotics Automation*, vol. 1, Apr. 2000, pp. 348-353.
- [3] A. Blake and M. Taylor, "Planning planar grasps of smooth contours," in *Proc. IEEE Int. Conf. Robotics Automation*, vol. 2, May 1993, pp. 834-839.
- [4] R. C. Brost and K. Goldberg, "A complete algorithm for designing planar fixtures using modular components," *IEEE Trans. Robot. Automat.*, vol. 12, pp. 31-46, Feb. 1996.
- [5] W. Cai, S. J. Hu, and J. X. Yuan, "Deformable sheet-metal fixturing: Principles, algorithms, and simulations," *Trans. ASME J. Manufact. Sci. Eng.*, vol. 118, no. 3, pp. 318-24, 1996.
- [6] J. F. Canny and K. Y. Goldberg, "'RISC' industrial robotics: Recent results and open problems," in *Proc. IEEE Int. Conf. Robotics Automation*, vol. 3, May 1994, pp. 1951-1958.
- [7] J. S. Carlson and R. Soderberg, "Assembly root cause analysis: A way to reduce dimensional variation in assembled products," *Int. J. Flexible Manufact. Syst.*, vol. 15, no. 2, pp. 113-150, 2003.
- [8] J.-S. Cheong, H. J. Haverkort, and A. F. van der Stappen, "On computing all immobilizing grasps of a simple polygon with few contacts," in *Proc. 14th Ann. Int. Symp. Algorithms and Computation*, Berlin, Germany, 2003.
- [9] D. Ding, G. Xiang, Y.-H. Liu, and W. M. Yu, "Fixture layout design for curved workpieces," in *Proc. IEEE Int. Conf. Robotics Automation*, vol. 3, May 2002, pp. 2906-2911.
- [10] K. Gopalakrishnan and K. Goldberg, "Gripping parts at concave vertices," in *Proc. IEEE Int. Conf. Robotics Automation*, vol. 2, May 2002, pp. 1590-1596.
- [11] K. Gopalakrishnan, M. Zaluzec, R. Koganti, P. Deneszczyk, and K. Goldberg, "Unilateral fixturing of sheet-metal parts using modular jaws with plane-cone contacts," in *Proc. IEEE Int. Conf. Robotics Automation*, vol. 3, Sept. 2003, pp. 3853-3858.
- [12] J. F. Hurtado and S. N. Melkote, "Effect of fixture design variables on fixture-workpiece conformability and static stability," in *Proc. IEEE/ASME Int. Conf. Advanced Intelligent Mechatronics*, vol. 1, July 2001, pp. 189-194.
- [13] H. Johannesson and R. Soderberg, "Structure and matrix models for tolerance analysis from configuration to detail design," *Res. Eng. Des.*, vol. 12, no. 2, pp. 112-125, 2000.

- [14] B. Li, B. W. Shiu, and K. J. Lau, "Robust fixture configuration design for sheet-metal assembly with laser welding," *J. Manufact. Sci. Eng.*, vol. 125, pp. 121–127, 2003.
- [15] —, "Fixture configuration design for sheet-metal assembly with laser welding: A case study," *Int. J. Adv. Manufact. Technol.*, vol. 19, no. 7, pp. 501–9, 2002.
- [16] H. F. Li, D. Ceglarek, and J. Shi, "A dexterous part-holding model for handling compliant sheet-metal parts, ASME transactions," *J. Manufact. Sci. Eng.*, vol. 124, no. 1, pp. 109–118, 2002.
- [17] X. Markenscoff, L. Ni, and C. H. Papadimitriou, "The geometry of grasping," *Int. J. Robot. Res.*, vol. 9, no. 1, pp. 61–74, 1990.
- [18] M. T. Mason, *Mechanics of Robotic Manipulation*. Cambridge, MA: MIT Press, 2001.
- [19] R. Menassa and W. De Vries, "Optimization methods applied to selecting support positions in fixture design," *ASME J. Eng. Ind.*, vol. 113, pp. 412–418, 1991.
- [20] B. Mishra, J. Schwarz, and M. Sharir, "On the existence and synthesis of multifinger positive grips," *Algorithmica* 2, vol. 2, pp. 541–558, 1987.
- [21] W. J. Plut and G. M. Bone, "3-D flexible fixturing using a multi-degree of freedom gripper for robotic fixtureless assembly," in *Proc. IEEE Int. Conf. Robotics Automation*, vol. 1, Apr. 1997, pp. 379–384.
- [22] —, "Limited mobility grasps for fixtureless assembly," in *Proc. IEEE Int. Conf. Robotics Automation*, vol. 2, Apr. 1996, pp. 1465–1470.
- [23] J. Ponce, J. Burdick, and E. Rimon, "Computing the immobilizing three-finger grasps of planar objects," in *Proc. 2nd Workshop Computational Kinematics*, 1995, pp. 281–300.
- [24] M. R. Rearick, S. J. Hu, and S. M. Wu, "Optimal fixture design for deformable sheet-metal workpieces," *Trans. NAMRI/SME*, vol. 21, pp. 407–412.
- [25] F. Reuleaux, *The Kinematics of Machinery*. New York: Macmillan, 1876.
- [26] E. Rimon and J. Burdick, "Mobility of bodies in contact—I," *IEEE Trans. Robot. Automat.*, vol. 14, pp. 696–708, 1998.
- [27] —, "On force and form closure for multiple finger grasps," in *Proc. IEEE Int. Conf. Robotics Automation*, vol. 2, Apr. 1996, pp. 1795–1800.
- [28] E. Rimon and A. Blake, "Caging planar bodies by one-parameter two fingered gripping systems," *Int. J. Robot. Res.*, vol. 18, no. 3, pp. 299–318, 1999.
- [29] Y. Rong and Y. Zhu, *Computer-Aided Fixture Design*. New York: Marcel Dekker, 1999.
- [30] Y. Rong and X.-S. Li, "Locating method analysis based rapid fixture configuration design," in *Proc. 6th Int. Conf. Emerging Technologies and Factory Automation*, 1997, pp. 27–32.
- [31] J. K. Salisbury, "Kinematics and force analysis of articulated hands," Ph.D. dissertation, Dept. Mech. Eng., Stanford Univ., Stanford, CA, 1982.
- [32] M. N. Sela, O. Gaudry, E. Dombre, and B. Benhabib, "A reconfigurable modular fixturing system for thin-walled flexible objects," *Int. J. Adv. Manufact. Technol.*, vol. 13, pp. 611–617, 1997.
- [33] B. W. Shiu, D. Apley, D. Ceglarek, and J. Shi, "Tolerance allocation for sheet-metal assembly using beam-based model," *Trans. IIE, Design Manufact.*, vol. 35, no. 4, pp. 329–342, 2003.
- [34] B. W. Shiu, D. Ceglarek, and J. Shi, "Flexible beam-based modeling of sheet-metal assembly for dimensional control," *Trans. NAMRI*, vol. 25, pp. 49–54, 1997.
- [35] P. Somoff, "Über gebiete von schraubengeschwindigkeiten eines starren körpers bievierschiedener zahl von stuz achen," *Z. Math. Phys.*, vol. 45, pp. 245–306, 1900.
- [36] A. F. van der Stappen, C. Wentink, and M. H. Overmars, "Computing form-closure configurations," in *Proc. IEEE Int. Conf. Robotics Automation*, vol. 3, May 1999, pp. 1837–1842.
- [37] R. Wagner, "Strut fixtures: Modular synthesis and efficient algorithms," Ph.D. dissertations, Comp. Sci. Dept., Univ. Southern California, Los Angeles, 1997.
- [38] M. Y. Wang and D. M. Pelinescu, "Optimizing fixture layout in a point-set domain," *IEEE Trans. Robot. Automat.*, vol. 17, pp. 312–323, June 2001.
- [39] M. Y. Wang, "Tolerance analysis for fixture layout design," *Assembly Automat.*, vol. 2, no. 2, pp. 153–162, 2002.
- [40] C. Xiong, Y. Rong, R. P. Koganti, M. J. Zaluzec, and N. Wang, "Geometric variation prediction in automotive assembling," *Assembly Automat.*, vol. 22, no. 3, pp. 169–260, 2002.



Kanakasabapathi Gopalakrishnan received the B.Tech. degree in mechanical engineering from the Indian Institute of Technology, Madras, India, in 2000. He is currently working toward the Ph.D. degree in industrial engineering and operations research at University of California, Berkeley.

He has worked on geometric and numerical algorithms for grasping/fixturing and part feeding, and is currently researching holding parts at concavities and holding deformable parts.

Mr. Gopalakrishnan is the recipient of numerous awards including a Bronze Medal at the 37th International Mathematics Olympiad and the Best Manipulation Paper award at the IEEE International Conference on Robotics and Automation, 2004.



Ken Goldberg (S'84–M'90–SM'98) received the undergraduate degree from the University of Pennsylvania, Philadelphia, in 1984, and the Ph.D. degree in computer science from Carnegie Mellon University, Pittsburgh, PA, in 1990. He also studied at Edinburgh University, Edinburgh, U.K., and the Technion, Israel.

From 1991 to 1995, he taught at University of Southern California, Los Angeles, and in Fall 2000 was Visiting Faculty at the Media Laboratory, Massachusetts Institute of Technology, Cambridge.

He is currently a Professor of Industrial Engineering and Operations Research and Electrical Engineering and Computer Science, University of California, Berkeley. He and his students work in two areas: geometric algorithms for automation and networked robots.

Dr. Goldberg received the National Science Foundation (NSF) Young Investigator Award in 1994, the NSF Presidential Faculty Fellowship in 1995, the Joseph Engelberger Award for Robotics Education in 2000, and the IEEE Major Educational Innovation Award in 2001. He is the Chair of the IEEE TRANSACTIONS ON AUTOMATION SCIENCE AND ENGINEERING Advisory Board.



Gary M. Bone received the B.Sc. (Ap.Sc.) degree in mechanical engineering from Queen's University, Kingston, ON, Canada, and the M.Eng. and Ph.D. degrees from McMaster University, Hamilton, ON, Canada in 1986, 1988, and 1993, respectively.

In 1994, he joined the Faculty of Engineering, McMaster University, where he is currently an Associate Professor in the Department of Mechanical Engineering. His research interests include flexible assembly, grasp and fixture planning, advanced control systems, pneumatic servo actuators, and

human-friendly robots.



Matthew J. Zaluzec received the B.S. degree in metallurgical engineering and the Ph.D. degree in materials science and engineering from the University of Illinois, Urbana-Champaign, in 1984 and 1990, respectively.

He is a Senior Staff Technical Specialist at Ford Motor Company's Research and Advanced Engineering Division, Dearborn, MI. He has 15 years of automotive materials and manufacturing experience and is currently the Advanced Manufacturing Technology Manager for the 2005 Ford GT Super Car.

His research focuses on advanced materials and manufacturing technology used in lightweight body architectures. He has presented and/or published over 60 technical papers covering advanced joining, coating, and manufacturing technologies.

Dr. Zaluzec has received numerous technical achievements awards within Ford Motor Company including the Henry Ford Technical Achievement award for his work on advanced aluminum materials for automotive applications. He has been awarded 28 U.S. Patents (95 patents worldwide) in areas encompassing advanced joining, high-performance coatings, materials and manufacturing processes for automotive applications. He serves on the Industrial Advisory Board of the Edison Welding Institute and is a member of ASM, ASME, and SAE.



Rama Koganti received the Bachelor's degree in mechanical engineering, the Master's degree in mechanical engineering from Concordia University, Montreal, QC, Canada, in 1993, and the Master's degree in industrial technology from Eastern Michigan University, Ypsilanti, MI.

He has been working at Ford Motor Company, Dearborn, MI, as a Technical Expert for over three years, in the area of light-weight body structures manufacturing processes (composite, aluminum, and ultralight steel materials). He has presented/pub-

lished more than 25 articles at various International Conferences, and journal transactions. Mr. Koganti serves as an Editorial Review Board Member for the *Quality Engineering Journal (ASQ)*, *Society of Automotive Engineers (SAE) Journal*, and the *Society of Manufacturing Engineers (SME) Journal*.

Rich Pearson received the B.S. degree in industrial engineering from San José State University, San José, CA, and the M.B.A. degree from the Michigan State University Executive Program, East Lansing.

He is the President and CEO of The National Center for Manufacturing Sciences, [(NCMS) the largest cross-industry collaborative manufacturing research consortium in the United States devoted exclusively to manufacturing technologies, process and practices], Ann Arbor, MI. Prior to his position at NCMS, he had a 38-year career with Ford Motor Company. Beginning as a draftsman/layout technician, he held a variety of manufacturing/process engineering and plant management positions in five Ford assembly plants. He also held Engineering Management positions at the corporate and division staff level. During his last assignment at Ford, he was the Manager of Technology Integration for the Advanced Manufacturing Engineering Division.



Patricia A. Deneszczuk received the B.S. degree in applied mathematics from Massachusetts Institute of Technology, Cambridge, MA, and the M.B.A. degree in operations management from the University of Michigan, Ann Arbor, in 1985.

She presently leads the Technology Integration activity at the Ford Motor Company, Dearborn, MI, managing advanced manufacturing technology development planning processes, ensuring consistency and alignment across manufacturing disciplines, as well as corporate strategic direction.

Ms. Deneszczuk is a member of the National Center for Manufacturing Sciences Board of Directors and the National Council for Advanced Manufacturing Leadership Forum.